Mathematics

AIMS Mathematics, 8(3): 7083–7096.
DOI: 10.3934/math.2023357
Received: 19 September 2022
Revised: 26 December 2022
Accepted: 29 December 2022
Published: 11 January 2023

http://www.aimspress.com/journal/Math

Research article

Moving average control chart under neutrosophic statistics

Muhammad Aslam[1,*], Khushnoor Khan[1], Mohammed Albassam[1] and Liaquat Ahmad[2]

[1] Department of Statistics, Faculty of Science, King Abdulaziz University, Jeddah 21551, Saudi Arabia
[2] Department of Statistics and Computer Science, University of Veterinary and Animal Sciences, Lahore 54000, Pakistan

* **Correspondence:** Email: aslam_ravian@hotmail.com.

Abstract: Continuous monitoring and improving the production process is a crucial step for the entrepreneur to maintain its position in the market. A successful process monitoring scheme depends upon the specification of the quality being monitored. In this paper, the monitoring of temperature is addressed using the specification of moving average under uncertainty. We determined the coefficients of the proposed chart utilizing the Monte Carlo simulation for a different measure of indeterminacy. The efficiency of the proposed chart has been evaluated by determining the average run lengths using several shift values. A real example of weather-related situation is studied for the practical adoption of the given technique. A comparison study shows that the proposed chart outperforms the existing chart in monitoring temperature-related data.

Keywords: control chart; process monitoring; temperature; neutrosophic statistics; Monte Carlo simulation; average run lengths
Mathematics Subject Classification: 62A86

1. Introduction

A control chart, a primary instrument for process monitoring, consists of a set of systematic procedures for observing and refining the quality of items produced through a process. The notion of a control chart was floated by Walter A. Shewhart, a physicist and statistician at Bell Laboratories, during 1920s. Since its inception, several techniques have been introduced by researchers for different conditions. A fast and quick indication by the chart refers to the efficient monitoring chart. Two types of variations are commonly threatened to the running process, first cause is negligible and no harmful to the production process whereas is known as the assignable cause which is harmful to the process [1], reporting the process as out-of-control and required to be identified quickly and fast corrective actions are crucial to rectify and streamline the process [2]. Control charts are constructed using three lines i.e., the lower control line (LCL), the upper control line (UCL) and a central line (CL).

In general, the control charts are presented for any monitoring phenomena consisting of a single observation but particular situations like interval values cannot be monitored using these techniques. For example, the data on the depth of water in a river cannot be expressed using the existing control chart techniques. To monitor the temperature variations in which the observations are collected in the form of intervals, Aslam [3] developed F-test to study interval data under discrete distribution.

The traditional Shewhart chart is relatively good for spotting big process shifts and is less popular in literature due to the incompetency to detect small process disturbances. In order to detect slight process shifts the researchers have proposed the exponentially weighted moving average (EWMA), cumulative sum (CUSUM) and moving average (MA) charts which are significantly delicate for smaller process shifts in the parameters of interest and achieved significant attention of the quality control researchers [4]. Due to the inertia problem, the detection capability of the EWMA chart is abhorrent among the quality control personals [4]. The CUSUM charts are tougher to apply and use than other control charts for detecting smaller shifts in the parameters. The MA charts are easy to understand and apply because it is created using simple averages but are slightly less efficient as compared to the EWMA and CUSUM charts whereas its collective working is relatively the same [5]. Chen and Yang [6] developed an MA chart for the continuous process failure mechanism. Wong et al. [5] suggested a simple MA chart as well as the joint Shewhart-MA chart. Khoo [7] proposed the MA chart for monitoring the number of non-conforming products. Khoo and Wong [8] suggested a double MA chart by measuring double moving averages and showed its efficiency over the simple MA on the basis of the average run lengths. Lin, Chou [9] designed an economic control chart using MA for auto-correlated observations. Maghsoodloo, Barnes [10] discussed the MA control chart and discussed their conditional average run length. More details on MA control charts can be seen in [11–14]. Knoth et al. [15] criticized modifications made to standard exponentially weighted moving average (EWMA) and cumulative sum (CUSUM) control charts. Abbas et al. [16] discussed some concerns raised on the auxiliary information-based control charts.

In recent years, neutrosophic statistics is being used very commonly by quality control researchers due to the nature of collected data which cannot be treated using traditional statistics [17]. The idea of neutrosophic statistics is based upon the fussy logic which considers the percentages of truth and falseness [18]. Several generalizations of fuzzy logic have been presented by [19–21]. Albassam, Khan [22] presented the application of D'Agostino test, a method used for evaluating the data, for neutrosophic statistics. In the real world, there are many situations in which exact, determined, certain, crisp or clear observations are not possible. For example, the depth of water in any river cannot be described in an exact figure but only the intervals of different areas can be stated. More references on neutrosophic can be appreciated in [17,19,23–30]. Woodall et al. [31] suggested that in the designing of the control charts under neutrosophic statistics, the sample size should not be imprecise.

However, little attention has been given to developing a control chart using the moving average scheme for the neutrosophic data which may attract the attention of several quality control experts. This paper attempts to introduce a charting scheme for dealing with neutrosophic statistic. The basic idea of this paper is to monitor the smaller variations in the uncertain data. The paper is arranged under different sections, appended below.

2. Materials and methods

Let the neutrosophic random variable is defined as $X_N = X_L + X_U I_N; I_N \epsilon [I_L, I_U]$ representing two parts X_L under traditional statistics and $X_U I_N; I_N \epsilon [I_L, I_U]$ representing the indeterminate part. Then neutrosophic random variable $X_N \epsilon [X_L, X_U]$ reduces to X_L when I_L=0. Let n presents the sample size. The mean of the neutrosophic ith subgroup can be described as $\bar{X}_{iN} \epsilon [\bar{X}_{iL}, \bar{X}_{iU}]$. Now we suppose that X_{ijN} belongs to the neutrosophic normal distribution with mean $\mu_N \epsilon [\mu_L, \mu_L]$ and variance $\sigma_N^2 \epsilon [\sigma_L^2, \sigma_U^2]$ respectively, for $i = 1,2, \ldots,$ and $j = 1,2, \ldots, n$. With reference to [2], NMA statistic is presented as

$$MA_{iN} = \frac{\bar{X}_{(i)N} + \bar{X}_{(i-1)N} + \cdots + \bar{X}_{(i-w+1)N}}{w}. \qquad (1)$$

Note that w presents span at time i. It can be observed that the statistic given in Eq (1) is parallel to (EWMA) statistic. The core modification is made for MA and EWMA schemes due to their sensitivity. Thus EWMA generates larger loads to the current observations whereas the MA provides an equal load to all observations, see [32].

2.1. Mathematical proofs

In this subsection, we will provide the mathematical proofs of the neutrosophic form of MA statistic, mean and variance of MA statistic, and control limits under neutrosophic statistics.

Suppose that $X_{iN} \epsilon [X_{iL}, X_{iU}]$ $(i = 1,2, \ldots)$ be a neutrosophic random variable having neutrosophic normal distribution with mean $\mu_N \epsilon [\mu_L, \mu_L]$ and variance $\sigma_N^2 \epsilon [\sigma_L^2, \sigma_U^2]$. Suppose that $\bar{X}_{iN} \epsilon [\bar{X}_{iL}, \bar{X}_{iU}]$ be the neutrosophic average of ith subgroup follows the neutrosophic normal distribution with mean $\mu_{0N} \epsilon [\mu_{0L}, \mu_{0L}]$ and variance $\sigma_N^2/n \, \epsilon [\sigma_L^2/n, \sigma_U^2/n]$, where n is a subgroup size. The neutrosophic form of $X_{iN} \epsilon [X_{iL}, X_{iU}]$ is expressed as

$$X_{iN} = X_{iL} + X_{iU} I_N; I_N \epsilon [I_L, I_U].$$

The neutrosophic form of $\bar{X}_{iN} \epsilon [\bar{X}_{iL}, \bar{X}_{iU}]$ is expressed as

$$\bar{X}_{iN} = \bar{X}_{iL} + \bar{X}_{iU} I_N; I_N \epsilon [I_L, I_U]$$

where the first values denote the determinate part, the second values denote indeterminate part and $I_N \epsilon [I_L, I_U]$ is a measure of indeterminacy.

The MA statistic under neutrosophic statistics when for $w = 3$ and $i = 4$ is expressed as

$$MA_{4N} = \frac{[\bar{X}_{4L}, \bar{X}_{4U}] + [\bar{X}_{3L}, \bar{X}_{3U}] + [\bar{X}_{2L}, \bar{X}_{2U}]}{3}$$

or

$$MA_{4N} = \frac{[\bar{X}_{4L} + \bar{X}_{4U} I_N] + [\bar{X}_{3L} + \bar{X}_{3U} I_N] + [\bar{X}_{2L} + \bar{X}_{2U} I_N]}{3}; \; I_N \epsilon [I_L, I_U]$$

or

$$MA_{4N} = \frac{\bar{X}_{4N} + \bar{X}_{3N} + \bar{X}_{2N}}{3}; \; I_N \epsilon [I_L, I_U].$$

In general, the MA statistic, say $MA_{iN} \epsilon [MA_{iL}, MA_{iU}]$ under neutrosophic can be expressed as follows:

$$MA_{iN} = \frac{\bar{X}_{(i)N}+\bar{X}_{(i-1)N}+\cdots+\bar{X}_{(i-w+1)N}}{w}.$$

Using the above-mentioned information, the neutrosophic form of the statistic $MA_{iN}\epsilon[MA_{iL}, MA_{iU}]$ can be expressed as

$$MA_{iN} = MA_{iL} + MA_{iU}I_N;\ I_N\epsilon[I_L, I_U].$$

Hence proved.
The mean of MA statistic under neutrosophic statistics is derived as follows:
We know

$$MA_{iN} = \frac{\bar{X}_{(i)N}+\bar{X}_{(i-1)N}+\cdots+\bar{X}_{(i-w+1)N}}{w}.$$

Applying expectation on both sides

$$E(MA_{iN}) = \frac{E(\bar{X}_{(i)N}) + E(\bar{X}_{(i-1)N}) + E(\bar{X}_{(i-2)N}) + \cdots + E(\bar{X}_{(i-w+1)N})}{w}$$

$$= \frac{\mu_{0N} + \mu_{0N} + \mu_{0N} + \cdots + \mu_{0N}}{w} = \frac{w\mu_{0N}}{w}$$

$$E(MA_{iN}) = \mu_{0N};\ \mu_{0N}\epsilon[\mu_{0L}, \mu_{0U}].$$

Hence proved.
The variance of MA_{iN} is derived as follows:
We know

$$MA_{iN} = \frac{\bar{X}_{(i)N}+\bar{X}_{(i-1)N}+\cdots+\bar{X}_{(i-w+1)N}}{w}.$$

Taking variance on both sides

$$V_N(MA_{iN}) = Var\left(\frac{\bar{X}_{(i)N} + \bar{X}_{(i-1)N} + \bar{X}_{(i-2)N} + \cdots + \bar{X}_{(i-w+1)N}}{w}\right)$$

$$V_N(MA_{iN}) = \frac{\sigma_N^2}{nw}; \sigma_N^2\epsilon[\sigma_L^2, \sigma_U^2].$$

Hence proved.
By definition, the lower control limit is defined by

$$LCL_N = E(MA_{iN}) - k\sqrt{V_N(MA_{iN})}$$

or

$$LCL_N = \mu_{0N} - k\sqrt{\frac{\sigma_N^2}{nw}};\ \mu_{0N}\epsilon[\mu_{0L}, \mu_{0U}], \sigma_N^2\epsilon[\sigma_L^2, \sigma_U^2].$$

By definition, the upper control limit is defined by

$$UCL_N = E(MA_{iN}) + k\sqrt{V_N(MA_{iN})}$$

or

$$UCL_N = \mu_{0N} + k\sqrt{\frac{\sigma_N^2}{nw}};\ \mu_{0N}\epsilon[\mu_{0L}, \mu_{0U}], \sigma_N^2\epsilon[\sigma_L^2, \sigma_U^2]$$

where k is the coefficient of control limits.

2.2. Design of the proposed chart

The neutrosophic form of $MA_{iN}\epsilon[MA_{iL}, MA_{iU}]$ is given by

$$MA_{iN} = MA_{iL} + MA_{iU}I_{NMA}; I_{NMA}\epsilon[I_{LMA}, I_{UMA}]. \quad (2)$$

The neutrosophic form of $MA_{iN}\epsilon[MA_{iL}, MA_{iU}]$ has two parts. The first part MA_{iL} presents the determinate part and $MA_{iU}I_{NMA}$ denote the indeterminate part and $I_{NMA}\epsilon[I_{LMA}, I_{UMA}]$ shows the measure of indeterminacy associated with $MA_{iN}\epsilon[MA_{iL}, MA_{iU}]$. Montgomery [2] presented the MA statistics which is the special case of $MA_{iN}\epsilon[MA_{iL}, MA_{iU}]$ and this neutrosophic form tends to MA_{iL} statistic if I_{LMA} =0. Then the mean and variance of the neutrosophic statistics $MA_{iN}\epsilon[MA_{iL}, MA_{iU}]$ for the in-control process i ≥ w; are given as

$$E_N(MA_{iN}) = \mu_{0N};\ MA_{iN}\epsilon[MA_{iL}, MA_{iU}],\ \mu_{0N}\epsilon[\mu_{0L}, \mu_{0U}] \quad (3)$$

and

$$V_N(MA_{iN}) = \frac{\sigma_N^2}{nw}; \sigma_N^2\epsilon[\sigma_L^2, \sigma_U^2]. \quad (4)$$

Under the above-stated process, the steps of suggested chart may be written as:
Step 1: Choose a sample having size n and w and calculate $MA_{iN}\epsilon[MA_{iL}, MA_{iU}]$.
Step 2: State the process in-control if $LCL_N \leq MA_{iN} \leq UCL_N$.
The functioning of the proposed control chart relay on the following pair of two neutrosophic control limits, given as

$$LCL_N = \mu_{0N} - k\sqrt{\frac{\sigma_N^2}{nw}}; \mu_{0N}\epsilon[\mu_{0L}, \mu_{0U}], \sigma_N^2\epsilon[\sigma_L^2, \sigma_U^2] \quad (5)$$

$$UCL_N = \mu_{0N} + k\sqrt{\frac{\sigma_N^2}{nw}};\ \mu_{0N}\epsilon[\mu_{0L}, \mu_{0U}], \sigma_N^2\epsilon[\sigma_L^2, \sigma_U^2]. \quad (6)$$

3. Monte Carlo simulation of the proposed neutrosophic statistic

In this section, the neutrosophic Monte Carlo (NMC) simulation of the neutrosophic MA chart has been presented. Let the mean of the in-control process be $\mu_{1N} = \mu_{0N} + c\sigma_N; \mu_{1N}\epsilon[\mu_{1L}, \mu_{1U}]$, here c is the introduced shift. The pre-specified average run length (ARL) for the smooth process is r_{0N}, further literature can be seen in [33]. The NMC simulation may be listed in the following steps, as:
Step-1: Generate neutrosophic observations of size n from the neutrosophic standard normal distribution with mean $\mu_{0N}\epsilon[\mu_{0L}, \mu_{0U}]$ and variance $\sigma_N^2\epsilon[\sigma_L^2, \sigma_U^2]$. Compute $\bar{X}_{iN}\epsilon[\bar{X}_{iL}, \bar{X}_{iU}]$ for ith subgroup.
Step-2: Calculate the statistic $MA_{iN}\epsilon[MA_{iL}, MA_{iU}]$ and show it on $LCL_N\epsilon[LCL_L, LCL_U]$ and $UCL_N\epsilon[UCL_L, UCL_U]$. Observe the first out-of-control number and note it as the run length.
Step-3: Run these steps 10,000 times and calculate ARL, say ARL_{0N} and neutrosophic standard deviation (NSD) of run-length. Select k with the condition that $ARL_{0N} \geq r_{0N}$.
Step-4: Generate neutrosophic observations of size n from the neutrosophic standard normal distribution with mean $\mu_{0N}\epsilon[\mu_{0L}, \mu_{0U}]$ and variance $\sigma_N^2\epsilon[\sigma_L^2, \sigma_U^2]$ at a specified shift c. Compute $\bar{X}_{iN}\epsilon[\bar{X}_{iL}, \bar{X}_{iU}]$ for ith subgroup.
Step-5: Calculate the value $MA_{iN}\epsilon[MA_{iL}, MA_{iU}]$ and show it on $LCL_N\epsilon[LCL_L, LCL_U]$ and

$UCL_N \epsilon [UCL_L, UCL_U]$. Observe the first out-of-control value which is known as the run length for the out-of-control process.

Step-6: Run the steps 10,000 spells and calculate ARL_{1N} and NSD for various values of c. Using the simulation process, ARL_{1N} and NSD for different values of c, n, I_N and w are computed and given in Tables 1–6. From Tables 1–6, the following findings related to ARL_{1N} are observed.

(1) The values of ARL_{1N} decreases as n increases when w is the same.

(2) The values of ARL_{1N} increases as r_{0N} increases from 300 to 370.

Table 1. The values of ARL when $r_{0N} = 200, n = 5, w = 3$.

c	k=2.742							
	I_N=0		I_N=0.02		I_N=0.05		I_N=0.10	
	ARL	NSD	ARL	NSD	ARL	NSD	ARL	NSD
0	200.46	196.06	172.90	172.37	141.53	140.77	99.89	95.75
0.1	129.68	129.02	111.52	108.54	92.79	90.17	70.73	67.82
0.2	58.23	56.69	51.86	49.90	44.14	42.19	35.60	33.73
0.3	28.10	26.03	25.15	23.38	22.23	20.33	18.50	16.74
0.4	15.14	13.47	14.22	12.28	13.08	11.06	11.13	9.26
0.5	9.43	7.55	9.00	7.13	8.28	6.38	7.35	5.44
0.6	6.49	4.53	6.16	4.27	5.86	3.91	5.36	3.37
0.7	4.86	2.79	4.71	2.70	4.51	2.44	4.26	2.18
0.8	3.99	1.86	3.91	1.71	3.80	1.61	3.64	1.36
0.9	3.50	1.17	3.46	1.13	3.40	1.04	3.29	0.86
1	3.24	0.74	3.21	0.67	3.18	0.62	3.13	0.53
2	3.00	0.00	3.00	0.00	3.00	0.00	3.00	0.00

Table 2. The values of ARL when $r_{0N} = 200, n = 10, w = 3$.

c	k =2.74							
	I_N=0		I_N=0.02		I_N=0.05		I_N=0.10	
	ARL	NSD	ARL	NSD	ARL	NSD	ARL	NSD
0	200.13	197.78	170.84	170.34	136.36	132.77	99.28	98.11
0.1	93.91	91.18	80.48	78.34	68.87	66.55	53.34	49.85
0.2	30.96	28.46	28.83	26.96	25.00	23.33	20.55	18.33
0.3	13.39	11.37	12.61	10.67	11.24	9.21	9.80	7.84
0.4	7.34	5.34	7.01	5.10	6.48	4.57	5.84	3.81
0.5	4.77	2.77	4.61	2.53	4.45	2.37	4.19	2.03
0.6	3.73	1.54	3.64	1.38	3.57	1.30	3.47	1.13
0.7	3.26	0.78	3.23	0.73	3.19	0.66	3.15	0.58
0.8	3.08	0.40	3.07	0.35	3.06	0.32	3.04	0.26
0.9	3.02	0.19	3.01	0.14	3.01	0.15	3.01	0.12
1	3.00	0.07	3.00	0.06	3.00	0.05	3.00	0.04
2	3.00	0.00	3.00	0.00	3.00	0.00	3.00	0.00

Table 3. The values of ARL when $r_{0N} = 300, n = 5, w = 3$.

c	k =2.879							
	I_N=0		I_N=0.02		I_N=0.05		I_N=0.10	
	ARL	NSD	ARL	NSD	ARL	NSD	ARL	NSD
0	302.90	293.75	253.53	248.34	200.54	197.20	140.70	137.32
0.1	184.48	184.07	159.40	157.93	130.94	129.59	95.52	94.19
0.2	78.14	75.84	70.22	68.19	57.82	54.70	45.02	42.92
0.3	36.40	34.61	32.83	30.77	28.12	26.45	22.53	20.53
0.4	18.63	16.58	17.12	15.00	15.25	13.38	12.97	11.14
0.5	10.92	9.01	10.27	8.22	9.48	7.59	8.44	6.57
0.6	7.31	5.45	7.01	5.15	6.50	4.63	5.89	3.93
0.7	5.37	3.35	5.12	3.12	4.89	2.89	4.52	2.41
0.8	4.22	2.11	4.15	2.00	3.98	1.82	3.77	1.54
0.9	3.65	1.38	3.57	1.27	3.49	1.15	3.41	1.02
1	3.30	0.86	3.29	0.83	3.22	0.70	3.17	0.62
2	3.00	0.00	3.00	0.00	3.00	0.00	3.00	0.00

Table 4. The values of ARL when $r_{0N} = 300, n = 10, w = 3$.

c	k =2.881							
	I_N=0		I_N=0.02		I_N=0.05		I_N=0.10	
	ARL	NSD	ARL	NSD	ARL	NSD	ARL	NSD
0	301.05	298.57	256.61	252.31	201.36	202.95	141.11	139.41
0.1	128.99	126.94	116.62	113.55	92.68	90.83	69.30	66.10
0.2	41.04	38.76	36.73	34.13	32.02	29.46	25.68	23.59
0.3	16.53	14.67	15.09	13.26	13.51	11.75	11.49	9.68
0.4	8.43	6.52	7.93	6.02	7.41	5.53	6.61	4.71
0.5	5.27	3.27	5.09	3.12	4.83	2.83	4.47	2.42
0.6	3.92	1.74	3.85	1.67	3.71	1.48	3.58	1.28
0.7	3.33	0.90	3.30	0.86	3.25	0.75	3.21	0.67
0.8	3.10	0.45	3.09	0.40	3.08	0.39	3.06	0.32
0.9	3.02	0.19	3.03	0.22	3.02	0.16	3.01	0.15
1	3.00	0.08	3.01	0.10	3.00	0.07	3.00	0.06
2	3.00	0.00	3.00	0.00	3.00	0.00	3.00	0.00

Table 5. The values of ARL when $r_{0N} = 370, n = 5, w = 3$.

c	k=2.948							
	I_N=0		I_N=0.02		I_N=0.05		I_N=0.10	
	ARL	NSD	ARL	NSD	ARL	NSD	ARL	NSD
0	369.58	357.26	312.20	307.10	247.69	246.41	167.04	164.08
0.1	219.99	215.32	187.81	183.44	153.03	151.02	110.04	109.85
0.2	90.94	89.49	81.11	78.02	67.33	65.26	51.51	49.77
0.3	39.91	37.63	36.50	34.17	30.94	28.92	25.16	23.18
0.4	20.90	19.04	18.75	16.93	16.89	14.95	14.21	12.17
0.5	11.92	9.97	11.15	9.24	10.06	8.19	8.80	6.97
0.6	7.88	5.96	7.49	5.51	6.90	4.98	6.12	4.22
0.7	5.63	3.65	5.36	3.35	5.07	3.07	4.71	2.69
0.8	4.39	2.32	4.29	2.23	4.07	1.93	3.91	1.72
0.9	3.73	1.51	3.66	1.40	3.57	1.28	3.46	1.14
1	3.37	0.97	3.32	0.89	3.28	0.80	3.21	0.69
2	3.00	0.00	3.00	0.00	3.00	0.00	3.00	0.00

Table 6. The values of ARL when $r_{0N} = 370, n = 10, w = 3$.

c	k=2.951							
	I_N=0		I_N=0.02		I_N=0.05		I_N=0.10	
	ARL	NSD	ARL	NSD	ARL	NSD	ARL	NSD
0	370.63	362.87	319.80	311.31	246.25	237.14	170.50	171.00
0.1	155.62	154.43	134.55	133.51	111.49	108.85	80.30	78.41
0.2	46.67	44.58	41.35	39.39	35.52	33.47	28.28	26.28
0.3	18.44	16.52	16.81	14.80	14.74	12.82	12.46	10.48
0.4	9.00	7.04	8.38	6.50	7.76	5.84	6.87	4.85
0.5	5.55	3.58	5.30	3.28	5.01	3.04	4.67	2.64
0.6	4.04	1.89	3.93	1.76	3.83	1.64	3.64	1.37
0.7	3.38	0.98	3.36	0.96	3.30	0.85	3.24	0.74
0.8	3.12	0.51	3.12	0.48	3.10	0.44	3.07	0.38
0.9	3.03	0.23	3.03	0.23	3.02	0.19	3.02	0.16
1	3.01	0.11	3.01	0.09	3.00	0.08	3.00	0.07
2	3.00	0.00	3.00	0.00	3.00	0.00	3.00	0.00

4. Results and discussion

In this section, ARL evaluation of the suggested NMA chart has been given with the parallel prevailing chart discussed by [2] under the classical statistics using the same parameters in terms of ARL_{1N}. For the fair comparison, we used similar values of r_{0N}, c, w and n.

4.1. Comparison of charts using ARL

Montgomery [2] discussed the MA chart under classical statistics. As mentioned earlier, the proposed control chart is the generalization of the existing MA chart. It is important to note that the proposed control chart reduces to the existing MA chart if no uncertainty is found in the observations. The ARLs are used for the evaluation and comparison of any proposed study [2]. It is worth mentioning here that a control chart having the least number of ARLs is considered the better or more capable chart as compared to a chart having larger ARLs. The values of ARL and NSD of the existing control chart mentioned by [2] when $I_N = 0$ are shown in the first column of Tables 1–6. From Tables 1–6, it can be seen that as the values of I_N increases, there is a decreasing trend in the values of ARL and NSD. For example, when $I_N = 0$ and c=0.2, from Table 5, the values of ARL and NSD are 90 and 89 and when $I_N = 0.02$ and c=0.2, from Table 5, the values of ARL and NSD are 81 and 80, respectively. This comparison shows that the proposed control chart gives smaller values of ARL and NSD as compared to the MA chart under classical statistics. Based on this information, it is concluded that the proposed control chart is more efficient than the control chart proposed by [2] under classical statistics.

4.2. Comparison using simulation data

Now, we compare the efficiency of the proposed chart with the existing control chart discussed by [2] under classical statistics using the simulated data. The data is generated from the neutrosophic normal distribution with $\mu_N \epsilon [0,0]$ and $\sigma_N^2 \epsilon [1,1]$. Forty neutrosophic observations are generated such that the first 20 neutrosophic observations are generated from the in-control process and the remaining neutrosophic observations are generated by considering c=0.4 and I_N=0.1. The values of $MA_{iL}$is computed and plotted on the control chart in Figure 1 (left) and the values MA_{iU} are computed and plotted on the control chart in Figure 1 (right). By comparing both figures in Figure 1, it can be noted that the values of MA_{iL}fall within the control limits that indicate that the process is in-control. On the other hand, the proposed control chart shows that the values of MA_{iU} go out the upper control limit at the 34th sample. Under an uncertain environment, the proposed control chart detects shift earlier than the control chart under classical statistics. The simulation study also shows the superiority of the proposed control chart over the existing control chart under classical statistics.

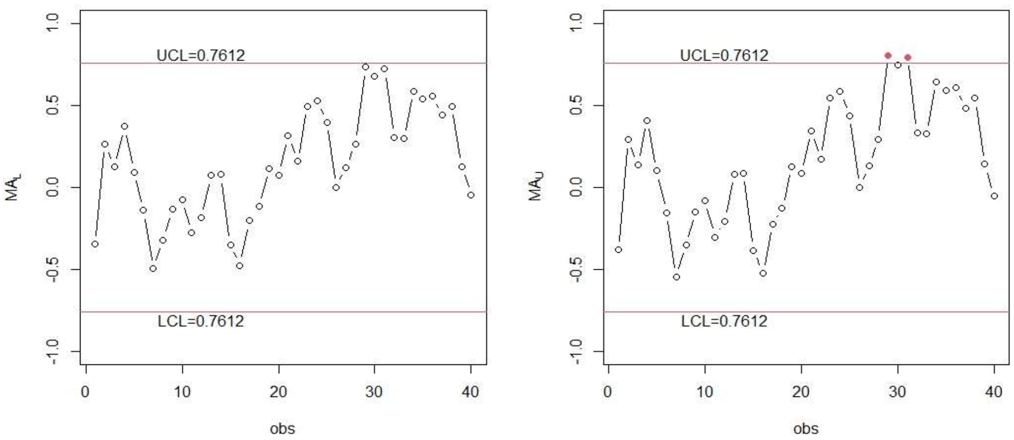

Figure 1. The existing and proposed control charts for simulated data.

5. Real world example

The study of the practical execution of the anticipated chart using the temperature data is included in the paper. For this purpose, the temperature data from the meteorological department of the Kingdom of Saudi Arabia have been collected and given in Table 7. The determinate (lower) values of temperature data of three times as morning, afternoon and evening of Jeddah city for the month of October 2019 have been collected from https://www.timeanddate.com/weather/saudi-arabia/jeddah/historic. The uncertainty/indeterminacy is always present in measuring the temperature data; see [34–36]. The upper value of the temperature data is calculated by supposing a measure of intermediacy, say $I_N = 0.1$. Under indeterminacy, the use of the existing control chart under classical statistics may mislead decision-makers. Therefore, the proposed control chart under indeterminacy should be designed for monitoring the temperature. The values of ARL and NAS for the real data are shown in Table 8. The values of neutrosophic statistic MA_{iN} are computed and plotted on the control chart in Figure 2. The left- hand side figure shows the MA control chart under classical statistics and the right-hand side figure shows the plot of the proposed control chart. On noticing Figure 2, it can be seen that all values of the statistic MA_{iL} falls within the control limit and indicate that the temperature is in-control. But the proposed control chart shows the shift in the temperature. We may conclude that the proposed chart displays some concerns about the temperature of the city as some points fall close to the upper control limit and the meteorologist should be alert whereas the classical chart shows fully in-control observations.

Table 7. The temperature data.

Weeks	Sample	AT 6 AM	12:00 PM	18 PM	MA_{iN}
Week 1 October 1	1	30	33	31	[31.33,34.47]
	2	30	33	31	[31.33,34.47]
	3	30	32	32	[31.33,34.47]
	4	30	32	30	[30.67,34.22]
	5	29	32	30	[30.33,33.86]
	6	29	33	32	[31.33,33.86]
	7	31	33	33	[32.33,34.47]
Week 2 October 8	1	31	35	31	[32.33,35.2]
	2	30	33	31	[31.33,35.2]
	3	31	32	31	[31.33,34.83]
	4	28	31	30	[29.67,33.86]
	5	29	32	31	[30.67,33.61]
	6	29	35	32	[32,33.86]
	7	30	32	31	[31,34.34]
Week 3 October 15	1	29	31	31	[30.33,34.22]
	2	28	33	30	[30.33,33.61]
	3	26	34	30	[30,33.24]
	4	27	32	31	[30,33.12]
	5	29	32	31	[30.67,33.24]
	6	28	31	29	[29.33,33]
	7	26	32	30	[29.33,32.76]

Continued on next page

Weeks	Sample	AT 6 AM	12:00 PM	18 PM	MA_{iN}
Week 4 October 22	1	28	31	29	[29.33,32.27]
	2	27	32	30	[29.67,32.39]
	3	27	32	30	[29.67,32.51]
	4	28	32	30	[30,32.76]
	5	29	32	29	[30,32.88]
	6	28	30	28	[28.67,32.51]
	7	26	30	28	[28,31.78]

Table 8. The values of ARL when $r_{0N} = 370, n = 3, w = 3$.

c	k=2.953							
	I_N=0		I_N=0.02		I_N=0.05		I_N=0.10	
	ARL	NSD	ARL	NSD	ARL	NSD	ARL	NSD
0	376.62	361.32	314.64	316.91	249.86	247.79	173.02	170.47
0.1	271.34	272.20	227.28	221.92	183.66	182.27	130.58	128.73
0.2	138.52	135.57	120.25	116.65	97.15	94.45	73.19	71.99
0.3	69.60	68.09	62.33	59.99	52.19	50.24	40.57	38.47
0.4	38.11	36.40	34.60	33.04	29.67	27.57	24.29	22.14
0.5	22.91	20.88	20.73	18.76	18.21	16.16	15.16	13.19
0.6	14.36	12.19	13.49	11.55	12.09	10.25	10.25	8.36
0.7	9.92	7.89	9.32	7.43	8.54	6.66	7.41	5.49
0.8	7.14	5.16	6.93	4.98	6.49	4.53	5.82	3.80
0.9	5.67	3.69	5.47	3.56	5.13	3.13	4.78	2.73
1	4.69	2.69	4.52	2.44	4.29	2.20	4.08	1.91
2	3.00	0.04	3.00	0.05	3.00	0.03	3.00	0.01

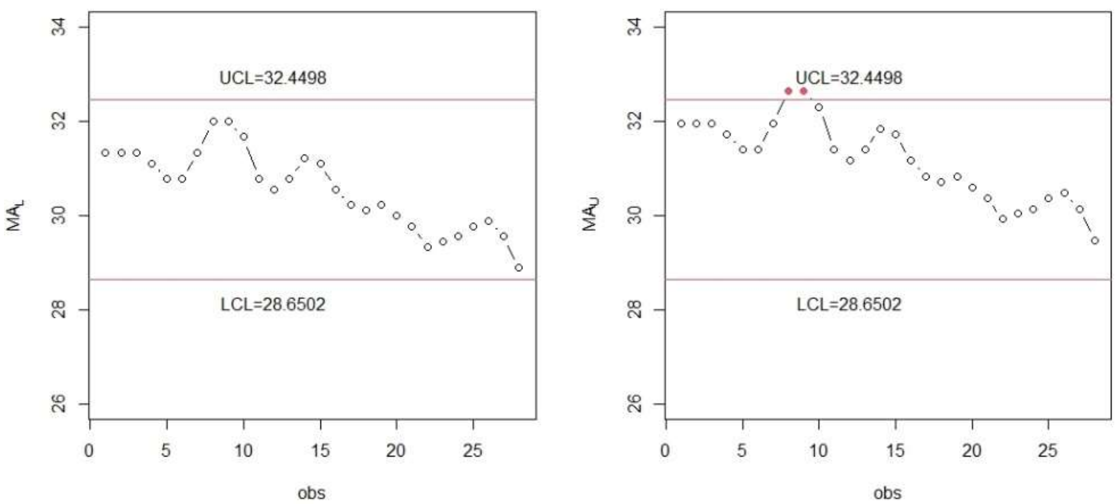

Figure 2. The existing and proposed control charts for temperature data.

By comparing the control charts in Figures 1 and 2, it can be seen that the control chart using simulated data in Figure 1 shows the out-of-control at the 34^{th} sample and the control chart using real data in Figure 2 shows the out-of-control at the 8^{th} sample.

6. Conclusions

In this paper, the neutrosophic moving average chart has been presented under the neutrosophic statistics. The coefficients of the charts have been computed for altered process situations. The average run length values have been calculated which show the better discovering ability of the suggested chart. The practical application of the suggested chart has been included by constructing the control chart under the proposed methodology for the temperature data. It has been concluded that the suggested chart is an effective chart using simulated and real data. The proposed control chart has the ability to detect shift earlier than the control chart using classical statistics. It has also been concluded that the suggested chart is a significant addition to the toolkit of the meteorologist. The suggested chart can be extended for the exponentially weighted moving averages using a resampling scheme for future research.

Acknowledgements

The authors are deeply thankful to the editor and reviewers for their valuable suggestions to improve the quality and presentation of the paper.

Conflict of interest

The authors declare no conflict of interest.

References

1. T. W. Nolan, L. P. Provost, Understanding variation, *Qual. Prog.*, **23** (1990), 70–78.
2. D. C. Montgomery, *Introduction to statistical quality control*, 6 Eds., New York: John Wiley & Sons, Inc, 2020.
3. M. Aslam, Neutrosophic statistical test for counts in climatology, *Sci. Rep.*, **11** (2021), 1–5. https://doi.org/10.1038/s41598-020-79139-8
4. W. P. Huang, L. J. Shu, Y. Su, An accurate evaluation of adaptive exponentially weighted moving average schemes, *IIE Trans.*, **46** (2014), 457–469. https://doi.org/10.1080/0740817X.2013.803642
5. H. Wong, F. F. Gan, T. Chang, Designs of moving average control chart, *J. Stat. Comput. Simul.*, **74** (2004), 47–62. https://doi.org/10.1080/0094965031000105890
6. Y. S. Chen, Y. M. Yang, An extension of Banerjee and Rahim's model for economic design of moving average control chart for a continuous flow process, *Eur. J. Oper. Res.*, **143** (2002), 600–610. https://doi.org/10.1016/S0377-2217(01)00341-1
7. M. B. Khoo, A moving average control chart for monitoring the fraction non-conforming, *Qual. Reliab. Eng. Int.*, **20** (2004), 617–635. https://doi.org/10.1002/qre.576
8. M. B. Khoo, V. Wong, A double moving average control chart, *Commun. Stat.-Simul. C.*, **37** (2008), 1696–1708. https://doi.org/10.1080/03610910701832459

9. S. N. Lin, C. Y. Chou, S. L. Wang, H. R. Liu, Economic design of autoregressive moving average control chart using genetic algorithms, *Expert Syst. Appl.*, **39** (2012), 1793–1798. https://doi.org/10.1016/j.eswa.2011.08.073
10. S. Maghsoodloo, D. Barnes, On moving average control charts and their conditional average run lengths, Wiley Online Library, **37** (2021), 3145–3156. https://doi.org/10.1002/qre.2992
11. S. Rachidi, E. Leclercq, Y. Pigne, D. Lefebvre, *Moving average control chart for the detection and isolation of temporal faults in stochastic Petri nets*, in 2018 IEEE 23rd International Conference on Emerging Technologies and Factory Automation (ETFA), IEEE, 2018. https://doi.org/10.1109/ETFA.2018.8502633
12. V. Alevizakos, K. Chatterjee, C. Koukouvinos, The triple moving average control chart, *J. Comput. Appl. Math.*, **384** (2021), 113171. https://doi.org/10.1016/j.cam.2020.113171
13. K. Talordphop, S. Sukparungsee, Y. Areepong, Performance of new nonparametric Tukey modified exponentially weighted moving average—Moving average control chart, *PloS One*, **17** (2022), e0275260. https://doi.org/10.1371/journal.pone.0275260
14. K. Raweesawat, S. Sukparungsee, Explicit formulas of arl on double moving average control chart for monitoring process mean of zipinar (1) model with an excessive number of zeros, *Appl. Sci. Eng. Prog.*, **15** (2022), 4588–4588. https://doi.org/10.14416/j.asep.2021.03.002
15. S. Knoth, N. A. Saleh, M. A. Mahmoud, H. Woodall, V. G. Tercero-Gómez, A critique of a variety of "memory-based" process monitoring methods, *J. Qual. Technol.*, 2022, 1–27. https://doi.org/10.1080/00224065.2022.2034487
16. N. Abbas, S. Ahmad, M. Riaz, Reintegration of auxiliary information based control charts, *Comput. Ind. Eng.*, **171** (2022), 108479. https://doi.org/10.1016/j.cie.2022.108479
17. U. Afzal, H Alrweili, N Ahamd, M Aslam, Neutrosophic statistical analysis of resistance depending on the temperature variance of conducting material, *Sci. Rep.*, **11** (2021), 1–6. https://doi.org/10.1038/s41598-020-79139-8
18. M. Aslam, M. Albassam, Presenting post hoc multiple comparison tests under neutrosophic statistics, *J. King Saud Univ.-Sci.*, **32** (2020), 2728–2732. https://doi.org/10.1016/j.jksus.2020.06.008
19. F. Smarandache, *Introduction to neutrosophic measure, neutrosophic integral, and neutrosophic probability*, Infinite Study, 2013.
20. F. Smarandache, *Neutrosophic logic-a generalization of the intuitionistic fuzzy logic*, Multispace & multistructure, Neutrosophic transdisciplinarity (100 collected papers of science), 2010, 396.
21. F. Smarandache, Neutrosophic set is a generalization of intuitionistic fuzzy set, Inconsistent intuitionistic fuzzy set (Picture Fuzzy Set, Ternary Fuzzy Set), Pythagorean fuzzy set, spherical fuzzy set, and q-rung orthopair fuzzy set, while neutrosophication is a generalization of regret theory, grey system theory, and three-ways decision (revisited), *J. New Theory*, **29** (2019), 1–31.
22. M. Albassam, N. Khan, M. Aslam, Neutrosophic D'Agostino test of normality: An application to water data, *J. Math.*, **2021** (2021). https://doi.org/10.1155/2021/5582102
23. C. Jana, M. Pal, A robust single-valued neutrosophic soft aggregation operators in multi-criteria decision making, *Symmetry*, **11** (2019), 110. https://doi.org/10.3390/sym11010110
24. A. A. A. Jarrín, D. S. P. Tamayo, S. A. M. Giler, J. C. A. Zambrano, D. M. Macazan, Neutrosophic statistics applied in social science, *Neutrosophic Sets Sy.*, **44** (2021).
25. M. Aslam, N. Khan, A new variable control chart using neutrosophic interval method-an application to automobile industry, *J. Intell. Fuzzy Syst.*, **36** (2019), 2615–2623. https://doi.org/10.3233/JIFS-181767
26. M. Aslam, N. Khan, M. Z. Khan, Monitoring the variability in the process using neutrosophic statistical interval method, *Symmetry*, **10** (2018), 562. https://doi.org/10.3390/sym10110562

27. T. Bera, N. K. Mahapatra, Introduction to neutrosophic soft groups, *Neutrosophic Sets Sy.*, **13** (2016), 118–127.
28. J. Chen, J. Ye, S. Du, Scale effect and anisotropy analyzed for neutrosophic numbers of rock joint roughness coefficient based on neutrosophic statistics, *Symmetry*, **9** (2017), 208. https://doi.org/10.3390/sym9100208
29. R. Alhabib, M. M. Ranna, H. Farah, Some neutrosophic probability distributions, *Neutrosophic Sets Sy.*, **22** (2018), 30–38.
30. M. Aslam, A. Al Shareef, K. Khan, RETRACTED ARTICLE: Monitoring the temperature through moving average control under uncertainty environment, *Sci. Rep.*, **10** (2020), 1–8. https://doi.org/10.1038/s41598-019-56847-4
31. W. H. Woodall, A. R. Driscoll, D. C. Montgomery, A review and perspective on neutrosophic statistical process monitoring methods, *IEEE Access*, **10** (2022), 100456–100462. https://doi.org/10.1109/ACCESS.2022.3207188
32. Z. Li, Z. Wang, Z. Wu, Necessary and sufficient conditions for non-interaction of a pair of one-sided EWMA schemes with reflecting boundaries, *Stat. Probabil. Lett.*, **79** (2009), 368–374. https://doi.org/10.1016/j.spl.2008.09.004
33. Z. Li, C. Zou, Z. Gong, Z. Wang, The computation of average run length and average time to signal: An overview, *J. Stat. Comput. Sim.*, **84** (2014), 1779–1802. https://doi.org/10.1080/00949655.2013.766737
34. D. B. Lobell, C. Bonfils, P. B. Duffy, Climate change uncertainty for daily minimum and maximum temperatures: A model inter-comparison, *Geophys. Res. Lett.*, **34** (2007). https://doi.org/10.1029/2006GL028726
35. M. Rischard, N. Pillai, K. A. McKinnon, Bias correction in daily maximum and minimum temperature measurements through Gaussian process modeling, *arXiv:1805.10214*, 2018. https://doi.org/10.48550/arXiv.1805.10214
36. R. G. Harrison, S. D. Burt, Quantifying uncertainties in climate data: Measurement limitations of naturally ventilated thermometer screens, *Environ. Res. Commun.*, **3** (2021), 061005. https://doi.org/10.1088/2515-7620/ac0d0b